Vibrational Sum-Frequency Spectroscopy of the Water Liquid/Vapor Interface†

B. M. Auer and J. L. Skinner*

Theoretical Chemistry Institute and Department of Chemistry, University of Wisconsin, Madison, Wisconsin 53706

Received: July 26, 2008; Revised Manuscript Received: October 10, 2008

We present theoretical calculations of the vibrational sum-frequency susceptibility for the water liquid/vapor interface. Our approach builds on previous calculations by us and others, using the time-averaging approximation within the mixed quantum/classical formulation for coupled vibrational chromophores, and electric-field maps for transition frequencies, dipoles, polarizabilities, and intramolecular vibrational couplings. We compare our results for the imaginary part of the susceptibility to those from recent experiments, and comment about the effects of intermolecular vibrational coupling and the assignment of features in the spectrum.

I. Introduction

Understanding the structure and dynamics of the water/air interface is important for many fields of science. Within the last 15 years, vibrational sum-frequency (VSF) spectroscopy has proven to be the most valuable experimental technique for probing structure and dynamics at interfaces,[1,2] and much experimental[3−15] and theoretical[16−30] work has been focused on the water/air interface. One controversial issue has to do with the molecular interpretation of the hydrogen-bonding region from 3000 to 3600 cm^{-1}, which has been attributed to "ice-like" and "water-like" molecules,[2,14] to the symmetric and antisymmetric stretch character of molecules in symmetric or asymmetric environments,[6,7,25] to a Fermi resonance between the symmetric stretch and the bend overtone,[15] to doubly hydrogen-bonded donor molecules with C_{2v} symmetry,[13] to mostly four-coordinated molecules,[31] or to mostly two-coordinated molecules.[26]

Our recent work[32,33] on Raman and infrared spectroscopy of neat H_2O, and earlier work of others,[7,28,34−40] shows that the effects of intermolecular vibrational coupling are substantial. In particular, instantaneous vibrational eigenstates of the liquid extend over up to 12 OH stretch chromophores and over up to 10 molecules.[32,33] Thus, interpretations of the liquid-state vibrational spectra based on vibrations and environments of individual molecules would appear to be questionable. It seems reasonable that intermolecular vibrational coupling is also important for VSF spectroscopy (VSFS) of the water/air interface, and this has been confirmed by recent theoretical calculations of Buch et al.[28]

One way to simplify the problem is to consider the OH stretch of dilute HOD in D_2O. The coupling between OH and OD local modes on the same HOD molecule has little effect because of the large frequency mismatch, rendering these two modes effectively uncoupled. The OH stretch is also effectively uncoupled from the OD stretches on the D_2O molecules, and thus, the OH stretch functions well as a local chromophore. This situation has been exploited to a significant extent in the steady-state and ultrafast spectroscopy of bulk water.[33] Analogously, the Richmond group has performed VSFS experiments on various mixtures of HOD, H_2O, and D_2O.[9,10] From their data, they were able to extract both the nonresonant and resonant susceptibilities. We believe that these experiments, especially in the limit of dilute HOD, together with theory and analysis, provide the most straightforward understanding of the structure and dynamics of the water/air interface.

We have recently calculated[29] the resonant VSF susceptibility for this case of dilute HOD in D_2O, finding good agreement with the experiments of Richmond and co-workers.[9,10] The calculations involved a mixed quantum/classical approach,[25−28,33,41] where the OH stretch was treated quantum mechanically, and all other nuclear degrees of freedom were treated classically. Non-Condon effects (the OH transition dipole and polarizability depend on the classical variables) and motional narrowing were included.[29] For this situation of isolated chromophores, it *is* possible to interpret the spectrum based on the molecular environments of individual molecules. We found that the dominant types of molecules contributing to the VSF susceptibility, in both the free-OH and hydrogen-bonding regions, were those with a single donor hydrogen bond and one or two acceptor hydrogen bonds.[29]

For the VSFS of neat H_2O, there remain (in our view) three questions: (1) Can one obtain good agreement with experiment using a generalization of the mixed quantum/classical approach used for HOD/D_2O? (2) If so, how important are the effects of intramolecular and (especially) intermolecular coupling? (3) Can one comment further on the assignment of the hydrogen-bonding region from 3000 to 3600 cm^{-1}? The goal of this paper is to attempt to answer these three questions. The mixed quantum/classical formulation for the vibrational spectroscopy of coupled chromophores has been developed,[17,28,40,42−53] as has the time-averaging approximation approach, which can speed up such calculations.[54,55] In addition, approximate ways of treating both the intramolecular and intermolecular coupling have been developed in the context of our recent theory of IR and Raman spectra for neat H_2O.[32,33] Thus, at this point, within this framework, the calculation of the resonant VSF susceptibility for water is relatively straightforward. Our model and calculations share many features with those described in the recent, comprehensive and excellent paper by Buch et al.[28]

II. Theory of VSFS for Coupled Vibrational Chromophores

In VSFS, an infrared light beam polarized in the $\hat{k}$ direction with frequency ω and a visible beam polarized in the $\hat{\jmath}$ direction

† Part of the special section "Aqueous Solutions and Their Interfaces".

10.1021/jp806644x CCC: $40.75
Published on Web 11/26/2008

with frequency ω' are incident on a sample. The polarization in the $\hat{\imath}$ direction with a frequency given by $\omega_S = \omega' + \omega$ is proportional to the second-order nonlinear susceptibility $\chi_{ijk}(\omega,\omega')$. The intensity of the scatttered light is therefore proportional to the squared magnitude of this susceptibility.

Microscopic expressions for $\chi_{ijk}(\omega,\omega')$ have been derived by several authors, and involve eight separate terms.[56,57] Two of these are called "resonant", since they are enhanced when ω is resonant with a vibrational transition, and the other six are called "nonresonant". The resonant terms are to a good approximation independent of ω', while the nonresonant terms are to a good approximation independent of ω. For fixed visible frequency, the nonresonant terms can be considered constant, and so one writes[1,56]

$$I(\omega) \sim |\chi^{\mathrm{R}}_{ijk}(\omega) + \chi^{\mathrm{NR}}_{ijk}|^2 \tag{1}$$

where $\chi^{\mathrm{R}}_{ijk}(\omega)$ and χ^{NR}_{ijk} are the resonant and nonresonant contributions, respectively. Of greatest interest is the absorptive part of the resonant response, $\mathrm{Im}[\chi^{\mathrm{R}}_{ijk}(\omega)]$, which in some instances can be extracted from the VSF intensity.[9,10] Alternatively, Shen and co-workers[12,14] have recently developed a phase-sensitive technique that allows for direct measurement of $\mathrm{Im}[\chi^{\mathrm{R}}_{ijk}(\omega)]$. In any case, this is the focus of our theoretical calculations.

The two terms contributing to the resonant part involve eigenstates of the matter Hamiltonian, which can be rewritten in terms of polarizability and dipole operators for the ground electronic state, and the eigenstates of the nuclear Hamiltonian. As in other branches of spectroscopy, this can then be rewritten in terms of quantum time-correlation functions.[58] Thus, we have[29]

$$\chi^{\mathrm{R}}_{ijk}(\omega) = i\int_0^\infty \mathrm{d}t\, \mathrm{e}^{i\omega t}\, \mathrm{Tr}[\rho \alpha_{ij}(t)\, \mu_k(0)] \tag{2}$$

where the trace is over all nuclear quantum states, ρ is the equilibrium density operator for the nuclear Hamiltonian, $\alpha_{ij}(t)$ is the appropriate tensor element of the time-dependent polarizability operator (in the Heisenberg representation) for the ground electronic state, and $\mu_k(t)$ is the appropriate vector component of the dipole operator for the ground electronic state.

This quantum time-correlation function cannot at present be evaluated for any realistic model of a liquid, which forces one to make additional approximations. The simplest such approximation involves replacing the quantum time-correlation function by its classical counterpart. For infrared light frequency ω with $\hbar\omega > kT$, this classical approximation will lead to substantial errors, and thus, it is important to multiply this result by a quantum correction factor.[23,59−61] To implement such a purely classical approach, one needs a simulation model with flexible molecules, and models for how the dipole moment and polarizability of the liquid depend on molecular coordinates. This is the approach taken by several authors.[18−24]

One issue that arises with the classical approach is that for OH stretch frequencies $\hbar\omega_{\mathrm{OH}} \gg kT$, which means that regions of the potential relevant for the $0 \rightarrow 1$ fundamental transition are significantly higher in energy than those sampled in a classical simulation. Second, the OH stretch potential is very anharmonic, suggesting that the harmonic or nearly harmonic frequencies associated with a classical simulation will be poor approximations to the actual transition frequencies. This issue has prompted theorists to adopt a mixed quantum/classical approach. For a system of coupled vibrational chromophores, each relevant stretch coordinate is treated quantum mechanically, and all other degrees of freedom are either kept rigid or treated classically. Thus, in this approach, the susceptibility is given by[29,32,54]

$$\chi^{\mathrm{R}}_{ijk}(\omega) \sim i\int_0^\infty \mathrm{d}t\, \mathrm{e}^{i\omega t} \sum_{ln} \langle a_{lij}(t)\, G_{ln}(t)\, m_{nk}(0)\rangle \mathrm{e}^{-t/2T_1} \tag{3}$$

where $a_{lij}(t)$ is tensor component ij of the transition polarizability for chromophore l (which is time-dependent because it depends on classical variables) and $m_{nk}(t)$ is vector component k of the transition dipole for chromophore n. $G_{ln}(t)$ are the elements of the propagator matrix $\mathbf{G}(t)$, which satisfies the equation

$$\dot{\mathbf{G}}(t) = -i\boldsymbol{\kappa}(t)\, \mathbf{G}(t) \tag{4}$$

subject to the initial condition that $G_{ln} = \delta_{ln}$, and with

$$\kappa_{ln}(t) = \omega_l(t)\delta_{ln} + \omega_{ln}(t)(1 - \delta_{ln}) \tag{5}$$

Thus, $\boldsymbol{\kappa}(t)$ is a matrix whose diagonal elements are the fluctuating transition frequencies, $\omega_l(t)$, and whose off-diagonal elements are the fluctuating couplings $\omega_{ln}(t)$. The angular brackets now denote a classical equilibrium average. The vibrational lifetime, T_1, has been added phenomenologically. It is taken to be a constant, but more realistically, it should be frequency-dependent, as molecules in different environments will have different lifetimes.

For a large number of coupled chromophores, it can be difficult to obtain adequate statistics using eq 3, which prompted the development of a time-averaging approximation (TAA),[54] in which a motionally narrowed line shape for an isolated chromophore is viewed as a distribution of time-averaged frequencies. In the TAA for coupled chromophores, we consider the time-averaged matrix

$$\boldsymbol{\kappa}_T = \frac{1}{T}\int_0^T \mathrm{d}t'\, \boldsymbol{\kappa}(t') \tag{6}$$

which depends parametrically on the averaging time T. For any one realization of the trajectory $\boldsymbol{\kappa}(t)$, $\boldsymbol{\kappa}_T$ is diagonalized by the orthogonal transformation $\mathbf{N}^T\boldsymbol{\kappa}_T\mathbf{N}$, and then, the susceptibility can be written approximately as[32,54]

$$\chi^{\mathrm{R}}_{ijk}(\omega) \sim \sum_n \left\langle \frac{p_n(T)\, d_n(0)}{\gamma_n - \omega - i/2T_1} \right\rangle \tag{7}$$

where

$$p_n(t) = \sum_l a_{lij}(t) N_{ln} \tag{8}$$

$$d_n(t) = \sum_l m_{lk}(t) N_{ln} \tag{9}$$

and γ_n are the eigenvalues of $\boldsymbol{\kappa}_T$.

It is also useful to consider the susceptibility in the inhomogeneous limit, in which case $\boldsymbol{\kappa}(t)$ can be replaced by its initial

value in eq 4, and so $\mathbf{G}(t) = e^{-i\kappa(0)t}$. In this limit, the susceptibility is

$$\chi^{R}_{ijk}(\omega) \sim \sum_n \left\langle \frac{q_n(0)\, c_n(0)}{\lambda_n(0) - \omega - i/2T_1} \right\rangle \tag{10}$$

where

$$q_n(0) = \sum_l a_{lij}(0) B_{ln} \tag{11}$$

$$c_n(t) = \sum_l m_{lk}(0) B_{ln} \tag{12}$$

$\mathbf{B}$ is the matrix that diagonalizes $\kappa(0)$, and $\lambda_n(0)$ are the eigenvalues of $\kappa(0)$. Note, also, that, in the limit of no coupling between chromphores, $B_{ln} = \delta_{ln}$ and thus eq 10 becomes[29]

$$\chi^{R}_{ijk}(\omega) \sim \sum_n \left\langle \frac{a_{nij}(0)\, m_{nk}(0)}{\omega_n(0) - \omega - i/2T_1} \right\rangle \tag{13}$$

In order to evaluate the above expressions within the context of a molecular dynamics (MD) simulation, we will use the methods developed earlier[29,32,33,54,62] to obtain transition frequencies, dipoles, and polarizabilities, and intramolecular and intermolecular couplings, for each configuration of the liquid slab in the course of the simulation. To recap briefly, electronic-structure-based maps give approximate relations for an OH chromophore's transition frequency, transition dipole, and isotropic transition polarizability, as a function of a component of the electric field due to the point charges on surrounding molecules.[54,62] The required components of the transition polarizability tensor are calculated using a bond polarizability model.[29,33] Intramolecular couplings were approximated by a similar electric-field map,[54,32] and intermolecular couplings are calculated using transition-dipole interactions.[32] Note that, in our latest work on vibrational spectra for the bulk liquid,[32] our map for the dipole derivative of an OH stretch is described in terms of the ratio μ'/μ'_g, where μ' is the dipole derivative and μ'_g is the derivative for the gas-phase molecule. For the calculation of the intermolecular couplings, one then needs to know the values of the dipole derivatives, and in this context, one needs the value for the gas-phase molecule, which we inadvertantly neglected to provide. Within the level of electronic structure theory described in that paper,[32] the value is $\mu'_g = 0.18749$ au.

III. Results

A. Molecular Dynamics Simulation. MD simulations of H_2O were performed using the SPC/E model.[63] To build the interface, a cubic box of 256 molecules at the experimental density of H_2O at 300 K was constructed. Periodic boundary conditions were employed, and the electrostatic forces were computed using an approximation to the Ewald sum.[64] The classical equations of motion were integrated with the leapfrog algorithm with a 1 fs time step,[65] and rotations were treated using quaternions.[66] Velocities were rescaled and equilibrated repeatedly until the desired temperature of 300 K was obtained. Once the box was equilibrated, the z dimension was tripled, producing a slab with two interfaces. The slab was equilibrated as above with the exception that the particle-mesh Ewald method was used to treat the electrostatics, since the box is no longer cubic. In this work, 10 different slabs were constructed, and each was run for 1 ns, producing a total simulation time of 10 ns.

At each time step in the simulation, the electric field on each H is computed using point charges from all other molecules within a cutoff of 7.831 Å.[29,32] From the electric fields, one obtains the transition frequencies, intramolecular couplings, isotropic transition polarizabilities, and the transition dipoles. The oxygen atom density profile (as a function of z, the coordinate normal to the surface) displayed the familiar hyperbolic tangent form,[29] and we define z^* to be the shifted coordinate such that $z^* = 0$ corresponds to the center of the interface (the Gibb's dividing surface).

B. Resonant Susceptibility. The resonant susceptibility is computed from eq 7, using an averaging time of $T = 76$ fs, the same value we used for the bulk.[32] Note that we could have optimized this averaging time for the surface, by comparing susceptibilities in the uncoupled case using the full motional-narrowing formula[29] and the TAA,[54] but we decided to forego this extra complication. Since we generate two interfaces, it is necessary to divide the slab into two halves. At each starting time when calculating κ_T, each molecule is assigned to either the top or bottom of the box based on the oxygen position. Then, κ_T is constructed and diagonalized for each half separately. Note that this procedure produces an artifact, in that molecules near the artificial dividing surface are not coupled to the full complement of neighboring molecules. Presumably, however, since the average symmetry of the molecules is such that away from the interface they do not contribute to the VSF signal, this does not lead to problems (as long as the typical spatial extent of the vibrational eigenstates is somewhat less than half the thickness of the slab).

A recent study by McGuire and Shen has shown that the population relaxation time T_1 for the free-OH bonds at the surface is 1.3 ps,[67] while a similar study shows that T_1 for the hydrogen-bonding region at the surface is 190 fs.[68] Thus, T_1 should depend on frequency. These values of T_1 lead to appreciable extra broadening only for the free-OH peak (since the hydrogen-bonding region is already so broad), and thus, in what follows, we take T_1 to be constant, with a value of 1.3 ps.

Most experiments to date have been performed with ssp polarization,[10,14] where the sum-frequency and visible beams are polarized perpendicular to the scattering plane and parallel to the surface, and the IR beam is polarized in the scattering plane.[1] The relevant tensor element of χ^R is then xxz or yyz.[1] In the experiments by Raymond et al.,[10] even though they measure the squared magnitude of the resonant susceptibility, through a careful study of systems with different ratios of H_2O and D_2O, they were able to fit the susceptibilities themselves, leading to a determination of the imaginary part (which contains all of the relevant molecular-level information) for H_2O. On the other hand, Ji et al.,[14] using a phase-sensitive technique, measure the imaginary part directly.

In Figure 1, we compare the imaginary component of the resonant susceptibility, $\mathrm{Im}[\chi^R_{xxz}(\omega)]$, calculated using eq 7, with that from experiment.[10,14] (The three curves are normalized to have the same height of the free-OH peak.) Except for an error in the theoretical position for the free-OH peak of about 30 cm^{-1} (which comes about since our frequency map was parametrized for bulk water rather than for the surface[29]), the agreement between theory and the experiment of Raymond et al. is excellent. The agreement between theory and the experiment of Ji et al. is not nearly as good; in particular, the theory misses

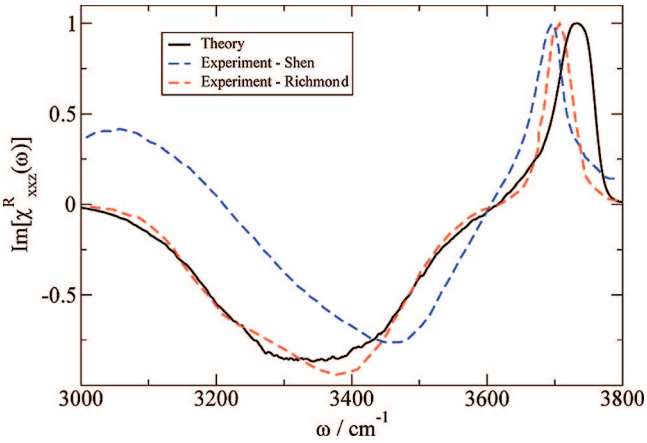

Figure 1. Imaginary part of the resonant susceptibility for ssp polarization, theory and experiment.[10,14]

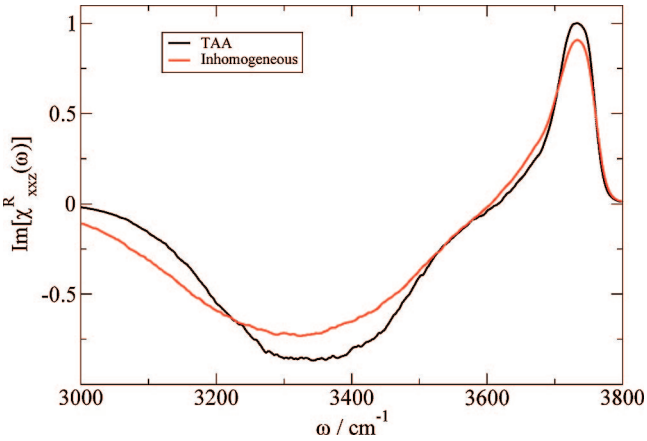

Figure 2. Imaginary part of the resonant susceptibility for ssp polarization, theory (using the TAA) and the inhomogeneous limit.

the positive feature in the experimental susceptibility below 3200 cm^{-1}. Regarding the disagreement between the experiments themselves, on the one hand, one would think that a direct measurement of the imaginary part[14] would be more reliable than using a fitting procedure to obtain it from the overall intensity.[10] On the other hand, it is possible that much of this disagreement arises from using different procedures for correcting for linear and nonlinear Fresnel coefficients and varying excitation laser characteristics especially at lower frequency.[10]

It is interesting to assess the extent of motional narrowing, by comparing the imaginary part of the TAA result for the susceptibility, eq 7, to the result in the inhomogeneous limit, eq 10, as shown in Figure 2. We see that motional narrowing produces a relatively modest 10 or 15% effect, which is slightly less than in the case of dilute HOD in D_2O.[29]

C. Effect of Vibrational Coupling. One of the goals of this paper is to understand how important intermolecular coupling is for water VSFS. To this end, it is convenient to consider the spectral density

$$W(\omega) = \sum_n \langle q_n(0)\, c_n(0)\, \delta(\omega - \lambda_n(0))\rangle \qquad (14)$$

which is the imaginary part of the resonant susceptibility in the inhomogeneous limit, eq 10, and in the limit that $T_1 \rightarrow \infty$. This frequency distribution, weighted by the collective transition dipoles and polarizabilities, can be viewed as the central quantity

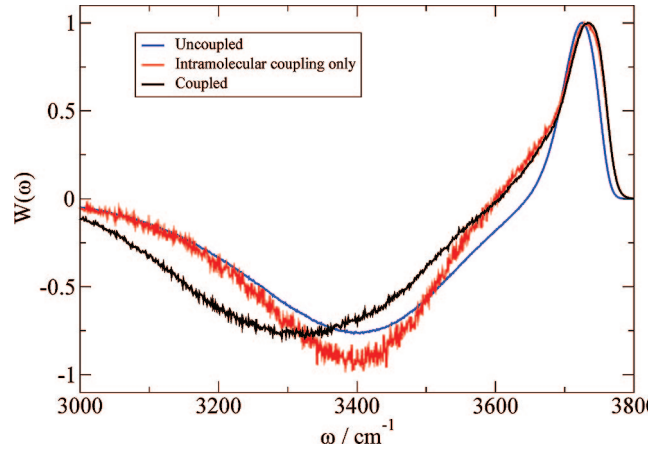

Figure 3. Spectral density for ssp polarization: theoretical results for the fully coupled system, the hypothetical system with intramolecular coupling only, and the hypothetical system with no vibrational coupling.

for VSFS for coupled systems. This spectral density is shown in Figure 3. One sees (comparing to Figure 1 or 2) that this spectral density is indeed similar to the imaginary part of the susceptibility. Next, we repeat the calculation but set all intermolecular coupling to zero (retaining the intramolecular coupling). This result is also shown in Figure 3. We see that neglect of this intermolecular coupling does not produce much change above 3600 cm^{-1} but does change the spectral density significantly below 3600 cm^{-1}. In particular, the peak in the spectral density shifts from 3300 to 3400 cm^{-1}, and the amplitude is reduced substantially below 3200 cm^{-1}. Thus, it is clear that for quantitative calculations one needs to include this coupling. One can also make a further comparison by considering the spectral density in the absence of all coupling, which is[29] (also see eq 13)

$$W(\omega) = \sum_n \langle a_{nij}(0)\, m_{nk}(0)\, \delta(\omega - \omega_n(0))\rangle \qquad (15)$$

This result (identical to that for HOD/D_2O[29]) is also shown in Figure 3. In addition to a decrease in the peak amplitude at 3400 cm^{-1}, removing the remaining intramolecular coupling makes a pronounced change between 3500 and 3700 cm^{-1}, presumably because in this region symmetry-breaking perturbations from the gas-phase local-mode frequencies are not large, and thus, the intramolecular coupling has a noticeable effect.

Another way to assess the effect of vibrational coupling is to consider the instantaneous eigenstates themselves, and especially their extent of delocalization. Thus, we focus on the inverse participation ratio,[32] as a function of frequency and position in the interface. To determine the latter, we define the center of probability for an instantaneous eigenstate, by $\sum_i \vec{r}_i |B_{in}|^2$, where the sum is over all OH stretches, $|B_{in}|^2$ is the probability of finding eigenstate n on OH stretch i (recall that $\mathbf{B}$ is the matrix that diagonalizes $\kappa(0)$), and $\vec{r}_i$ is the position of the oxygen atom involved in OH stretch i. For each eigenstate, we can then calculate the inverse participation ratio, given by

$$R_n = \left(\sum_i |B_{in}|^4\right)^{-1} \qquad (16)$$

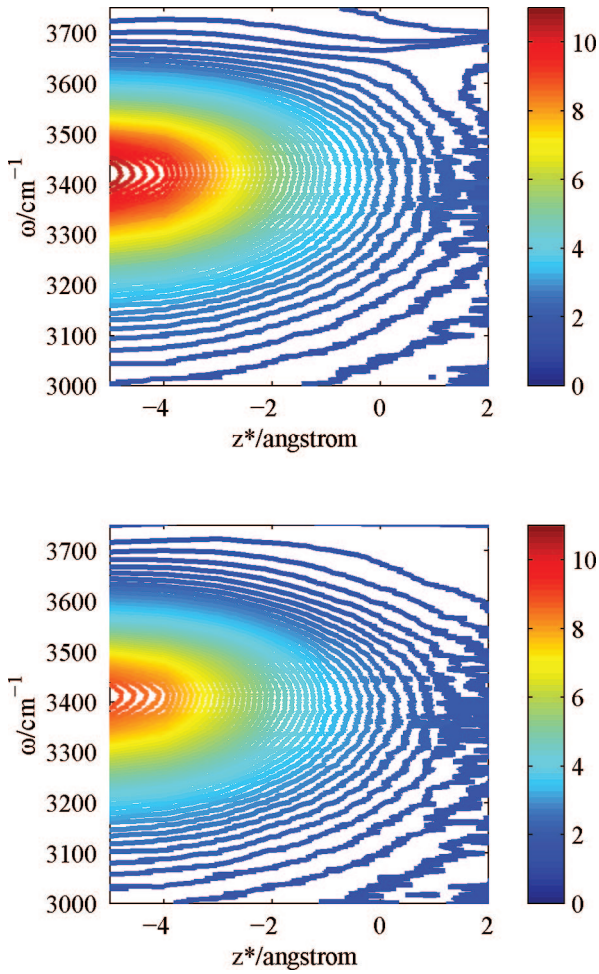

Figure 4. Inverse participation ratio (top panel) and molecular inverse participation ratio (bottom panel), as a function of position in the interface and frequency.

which is a way of quantifying over how many OH stretches each eigenstate extends. This ratio can be averaged over eigenstates within a narrow frequency window, and whose center of probability is within a narrow spatial window a distance z^* from the center of the interface.

Thus, in Figure 4 (top panel), we show a contour plot of this inverse participation ratio as a function of ω and z^*. Well into the slab, at $z^* = -5$ Å, R reaches a maximum of over 10 at about 3400 cm^{-1}, which is very similar to what we[32] and Buch et al.[28] observed for bulk water. As one approaches the interface, R decreases, as there are fewer OH stretches to couple with, and it is of interest to understand over how many OH stretches the eigenstates that participate in the VSF spectrum extend. In this context, it is useful to consult Figure 10 of our paper on dilute HOD in D_2O,[29] which shows that in the hydrogen-bonding region the maximum contribution comes from molecules about 0.5 Å inside the center of the interface. Correspondingly, then, from Figure 4, we see that, at $z^* = -0.5$ Å and $\omega = 3400$ cm^{-1}, R is above 3. Moreover, molecules as far as 2 Å inside the interface still make a sizable contribution to the spectrum, and for these molecules, R is about 6. In the free-OH region (see again Figure 10 of our HOD/D_2O paper[29]), the maximum contribution to the spectrum comes from molecules right at the center of the interface. Thus, from Figure 4, we see that, at $z^* = 0$ Å and $\omega = 3700$ cm^{-1}, R is just over 1. Therefore, in this region, the eigenstates are localized on individual OH chromophores.

It is also of interest to determine, on average, if the eigenstates extend primarily over OH groups on different molecules or over both OH groups on each involved molecule. We previously defined a molecular inverse participation ratio for each eigenstate n by[32]

$$R_{mn} = \left(\sum_{\alpha} \left\{ \sum_{\beta=1}^{2} |B_{\alpha\beta n}|^2 \right\}^2 \right)^{-1} \tag{17}$$

where α runs over all molecules in the half-box and β indexes the two OH stretches on each molecule. A contour plot of this quantity is shown in the lower panel of Figure 4. One sees quite generally that, for each frequency and distance, R_m is only slightly smaller than R, meaning that, if an eigenstate extends over R OH chromophores, it also extends more or less over R (rather than $R/2$) molecules! A similar situation was found for the bulk.[32]

V. Conclusion

Using theoretical methods developed for infrared and Raman spectroscopy in bulk water, and for VSFS of dilute HOD in D_2O, including a mixed quantum/classical formulation, various electric-field maps, and the time-averaging approximation, we have calculated the resonant susceptibility of the water liquid/vapor interface. In addition to the long list of possible theoretical deficiencies in our calculations of VSFS for dilute HOD in D_2O, discussed earlier[29] and which will not be recapitulated, one can worry about the adequacy of the approximations we have invoked for both intramolecular and intermolecular coupling, the time-averaging approximation we have used to calculate the susceptibility, and the use of the averaging time obtained from studies of bulk water. Here, however, we will focus on summarizing answers to the three questions we raised in the Introduction.

Regarding the agreement between theory and experiments from two different groups for the imaginary part of the susceptibility, we first note that the experimental results themselves are not in agreement. We believe that it is important to resolve this issue as soon as possible, as these experiments are important benchmarks that we theorists need in order to develop models and approaches. In fact, our theory is in excellent agreement with the experiment of Raymond et al.[10] but is not in good agreement with the experiment of Ji et al.[14] Given the many approximations made in modeling the water surface and the VSFS, tempting as it might be, it is probably not appropriate to use theory as a guide to assess which experiment is more correct.

Regarding the issue of vibrational coupling, by considering appropriate spectral densities with and without intra- and intermolecular coupling, and by considering the inverse participation ratio and its molecular variant, we conclude that, even near the center of the interface, from which comes the dominant contribution to the VSFS,[29] vibrational eigenstates extend over up to three molecules. Thus, we find that for quantitative calculations intramolecular, and especially intermolecular, vibrational coupling is important.

A corollary is that, since vibrational eigenstates extend over several molecules, even at the interface, one cannot with confidence assign features in the VSF intensity for H_2O to vibrations and environments of individual molecules. Note that, for dilute HOD in D_2O, for which vibrational coupling is presumably not an issue, we *can* attempt to make such assignments. Thus, it seems that for H_2O the best we can do is use the information from the isotope experiments, together with an understanding of how the collective effects of vibrational

coupling shift and enhance certain spectral regions, in much the same spirit as we did for IR and Raman spectra of the bulk liquid.[32,33] In particular, then, we believe that the intensity in the broad hydrogen-bonding region from 3000 to 3600 cm^{-1} arises from single-donor molecules making a total of two or three hydrogen bonds,[29] whose collective excitations are enhanced and red-shifted from their absorptions when vibrational coupling is neglected (or, for example, in dilute HOD in D_2O).

Acknowledgment. We are grateful for support from the National Science Foundation, through grant CHE-0750307. We thank Geri Richmond, Ron Shen, and Victoria Buch for helpful discussions.

References and Notes

(1) Richmond, G. *Chem. Rev.* **2002**, *102*, 2693.
(2) Shen, Y. R.; Ostroverkhov, V. *Chem. Rev.* **2006**, *106*, 1140.
(3) Du, Q.; Superfine, R.; Freysz, E.; Shen, Y. R. *Phys. Rev. Lett.* **1993**, *70*, 2313.
(4) Du, Q.; Freysz, E.; Shen, Y. R. *Science* **1994**, *264*, 826.
(5) Schnitzer, C.; Baldelli, S.; Campbell, D. J.; Schultz, M. J. *J. Phys. Chem. A* **1999**, *103*, 6383.
(6) Shultz, M. J.; Baldelli, S.; Schnitzer, C.; Simonelli, D. *J. Phys. Chem. B* **2002**, *106*, 5313.
(7) Liu, D.; Ma, G.; Levering, L. M.; Allen, H. C. *J. Phys. Chem. B* **2004**, *108*, 2252.
(8) Brown, M. G.; Raymond, E. A.; Allen, H. C.; Scatena, L. F.; Richmond, G. L. *J. Phys. Chem. A* **2000**, *104*, 10220.
(9) Raymond, E. A.; Tarbuck, T. L.; Richmond, G. L. *J. Phys. Chem. B* **2002**, *106*, 2817.
(10) Raymond, E. A.; Tarbuck, T. L.; Brown, M. G.; Richmond, G. L. *J. Phys. Chem. B* **2003**, *107*, 546.
(11) Wei, X.; Shen, Y. R. *Phys. Rev. Lett.* **2001**, *86*, 4799.
(12) Ostroverkhov, V.; Waychunas, G. A.; Shen, Y. R. *Phys. Rev. Lett.* **2005**, *94*, 046102.
(13) Gan, W.; Wu, D.; Zhang, Z.; Feng, R.; Wang, H. *J. Chem. Phys.* **2006**, *124*, 114705.
(14) Ji, N.; Ostroverkhov, V.; Tian, C. S.; Shen, Y. R. *Phys. Rev. Lett.* **2008**, *100*, 096102.
(15) Sovago, M.; Campen, R. K.; Wurpel, G. W. H.; Müller, M.; Bakker, H. J.; Bonn, M. *Phys. Rev. Lett.* **2008**, *100*, 173901.
(16) Benjamin, I. *Phys. Rev. Lett.* **1994**, *73*, 2083.
(17) Buch, V. *J. Phys. Chem. B* **2005**, *109*, 17771.
(18) Morita, A.; Hynes, J. T. *J. Phys. Chem. B* **2002**, *106*, 673.
(19) Morita, A. *J. Phys. Chem. B* **2006**, *110*, 3158.
(20) Perry, A.; Ahlborn, H.; Space, B.; Moore, P. B. *J. Chem. Phys.* **2003**, *118*, 8411.
(21) Perry, A.; Neipert, C.; Ridley, C.; Space, B.; Moore, P. B. *Phys. Rev. E* **2005**, *71*, 050601.
(22) Perry, A.; Neipert, C.; Kasprzyk, C. R.; Green, T.; Space, B.; Moore, P. B. *J. Chem. Phys.* **2005**, *123*, 144705.
(23) Perry, A.; Neipert, C.; Space, B.; Moore, P. B. *Chem. Rev.* **2006**, *106*, 1234.
(24) Brown, E.; Mucha, M.; Jungwirth, P.; Tobias, D. J. *J. Phys. Chem. B* **2005**, *109*, 7934.
(25) Morita, A.; Hynes, J. T. *Chem. Phys.* **2000**, *258*, 371.
(26) Walker, D. S.; Hore, D. K.; Richmond, G. L. *J. Phys. Chem. B* **2006**, *110*, 20451.
(27) Walker, D. S.; Richmond, G. L. *J. Phys. Chem. C* **2007**, *111*, 8321.
(28) Buch, V.; Tarbuck, T.; Richmond, G. L.; Groenzin, H.; Li, I.; Schultz, M. J. *J. Chem. Phys.* **2007**, *127*, 204710.
(29) Auer, B.; Skinner, J. L. *J. Chem. Phys.*, in press.
(30) Noah-Vanhoucke, J.; Smith, J. D.; Geissler, P. L. *J. Phys. Chem. B*, in press.
(31) Scatena, L. F.; Brown, M. G.; Richmond, G. L. *Science* **2001**, *292*, 908.
(32) Auer, B.; Skinner, J. L. *J. Chem. Phys.* **2008**, *128*, 224511.
(33) Skinner, J. L.; Auer, B. M.; Lin, Y.-S. *Adv. Chem. Phys.* **2008**, *000*, 000.
(34) Green, J. L.; Lacey, A. R.; Sceats, M. G. *J. Phys. Chem.* **1986**, *90*, 3958.
(35) Hare, D. E.; Sorensen, C. M. *J. Chem. Phys.* **1992**, *96*, 13.
(36) Falk, M.; Ford, T. A *Can. J. Chem.* **1966**, *44*, 1699.
(37) Belch, A.; Rice, S. *J. Chem. Phys.* **1983**, *78*, 4817.
(38) Rice, S.; Bergren, M.; Belch, A.; Nielson, N. *J. Phys. Chem.* **1983**, *87*, 4295.
(39) Wall, T. T.; Hornig, D. F. *J. Chem. Phys.* **1965**, *43*, 2079.
(40) Torii, H. *J. Phys. Chem. A* **2006**, *110*, 9469.
(41) Corcelli, S. A.; Lawrence, C. P.; Skinner, J. L. *J. Chem. Phys.* **2004**, *120*, 8107.
(42) l. C Jansen, T.; Zhuang, W.; Mukamel, S. *J. Chem. Phys.* **2004**, *121*, 10577.
(43) l C Jansen, T.; Dijkstra, A. G.; Watson, T. M.; Hirst, J. D.; Knoester, J. *J. Chem. Phys.* **2006**, *125*, 044312.
(44) lC Jansen, T.; Knoester, J. *J. Phys. Chem. B* **2006**, *110*, 22910.
(45) Mukamel, S.; Abramavicius, D. *Chem. Rev.* **2004**, *104*, 2073.
(46) Zhuang, W.; Abramavicius, D.; Hayashi, T.; Mukamel, S. *J. Phys. Chem. B* **2006**, *110*, 3362.
(47) Choi, J.; Hahn, S.; Cho, M. *Int. J. Quantum Chem* **2005**, *104*, 616.
(48) Oxtoby, D. W.; Levesque, D.; Weis, J.-J. *J. Chem. Phys.* **1978**, *68*, 5528.
(49) Everitt, K. F.; Lawrence, C. P.; Skinner, J. L. *J. Phys. Chem. B* **2004**, *108*, 10440.
(50) Hahn, S.; Ham, S.; Cho, M. *J. Phys. Chem. B* **2005**, *109*, 11789.
(51) Choi, J.-H.; Lee, H.; Lee, K.-K.; Hahn, S.; Cho, M. *J. Chem. Phys.* **2007**, *126*, 045102.
(52) Buch, V.; Bauerecker, S.; Devlin, J. P.; Buck, U.; Kazimirski, J. K. *Int. Rev. Phys. Chem.* **2004**, *23*, 375.
(53) Gorbunov, R. D.; Nguyen, P. H.; Kobus, M.; Stock, G. *J. Chem. Phys.* **2007**, *126*, 054509.
(54) Auer, B.; Skinner, J. L. *J. Chem. Phys.* **2007**, *127*, 104105.
(55) l. C. Jansen, T.; Ruszel, W. M. *J. Chem. Phys.* **2008**, *128*, 214501.
(56) Shen, Y. R. *The Principles of Nonlinear Optics*; Wiley-Interscience: Hoboken, NJ, 2003.
(57) Boyd, R. W. *Nonlinear Optics: Second Edition*; Elsevier: 2003.
(58) Gordon, R. G. *Adv. Magn. Reson.* **1968**, *3*, 1.
(59) Berens, P. H.; White, S. R.; Wilson, K. R. *J. Chem. Phys.* **1981**, *75*, 515.
(60) Bader, J. S.; Berne, B. J. *J. Chem. Phys.* **1994**, *100*, 8359.
(61) Egorov, S. A.; Everitt, K. F.; Skinner, J. L. *J. Phys. Chem. A* **1999**, *103*, 9494.
(62) Auer, B.; Kumar, R.; Schmidt, J. R.; Skinner, J. L. *Proc. Natl. Acad. Sci. U.S.A.* **2007**, *104*, 14215.
(63) Berendsen, H. J. C.; Grigera, J. R.; Straatsma, T. P. *J. Phys. Chem.* **1987**, *91*, 6269.
(64) Adams, D. J.; Dubey, G. S. *J. Comput. Phys.* **1987**, *72*, 156.
(65) Allen, M. P.; Tildesley, D. J. *Computer Simulation of Liquids*; Clarendon: Oxford, U.K., 1987.
(66) Svanberg, M. *Mol. Phys.* **1997**, *92*, 1085.
(67) McGuire, J. A.; Shen, Y. R. *Science* **2006**, *313*, 1945.
(68) Smits, M.; Ghosh, A.; Sterrer, M.; Müller, M.; Bonn, M. *Phys. Rev. Lett.* **2007**, *98*, 098302.

JP806644X